International Journal of Mass Spectrometry 313 (2012) 68–72

Contents lists available at SciVerse ScienceDirect

International Journal of Mass Spectrometry

journal homepage: www.elsevier.com/locate/ijms

Short communication

Mechanisms responsible for inducing and balancing the presence of Cs adatoms in dynamic Cs based SIMS

Klaus Wittmaack*

Helmholtz Zentrum München, Institute of Radiation Protection, 85758 Neuherberg, Germany

ARTICLE INFO

Article history:
Received 2 November 2011
Received in revised form 9 December 2011
Accepted 9 December 2011
Available online 5 January 2012

Keywords:
Secondary ion mass spectrometry
Cs bombardment
Adatom formation
Bond strength

ABSTRACT

Secondary ion mass spectrometry (SIMS) is an established technique for sensitive compositional analysis of solids. To achieve high sensitivity in the so-called dynamic SIMS mode, notably in the analysis of negative secondary ions, it is common practice to use Cs primary ions for sputter erosion as well as for loading the sample with Cs. In qualitative terms, the negative-ion yield enhancement has been attributed to a lowering of the sample's work function but, remarkably, the physical processes involved in producing the favorable conditions have not been clarified in any detail before. This study provides evidence that work function changes observed under Cs bombardment can be explained if the implanted ions are transiently converted to adatoms. Previously disregarded properties of Cs atoms include the huge size, the high mobility and bond formation with coverage dependent strength. It is shown that implanted Cs atoms are rapidly relocated towards the receding surface, presumably in response to the stress generated by the retained material. After passage through the solid–vacuum interface, Cs atoms loose their valance electron and become bound to the surface via dipole interaction. This way they become adatoms. Stationary conditions in terms of Cs surface coverage are established by the balance between adatom formation and sputter ejection at energies exceeding the bond strength. Combining calculated sputter cross sections for adatom removal with experimental data from various sources, the rates of Cs implantation and reemission are shown to be in balance with an uncertainty of only about ± 20%.

1. Introduction

Deposition of alkali atoms on solid surfaces is known to cause a significant or even large lowering of the work function [1]. In secondary ion mass spectrometry (SIMS), reduced work functions are commonly assumed to be responsible for the high yields of negative ions [2] as well as for the reduced yields of positive ions [3]. Such yield changes were observed when sub-monolayer quantities of Li or Cs were deposited on samples subsequently exposed to low-fluence ion bombardment, i.e., under conditions causing minimum distortion of the adatom layer [2,3]. Routine SIMS analysis, however, involves high-fluence sputter erosion of the sample to depths up to the micrometer range, commonly referred to as dynamic SIMS. High yields in dynamic SIMS may be obtained by simultaneously exposing the sample to a jet of Cs vapor and non-Cs energetic primary ions, e.g., Ga^+ [4,5]. Particularly high levels of sample loading with Cs are achieved by simultaneous exposure to a Cs jet and Cs^+ ions [5]. A more common approach is sample bombardment with a stand-alone Cs^+ ion beam [6–9]. Early studies showed that secondary ion yields of impurity or dopant elements depend strongly on the matrix in which they are embedded [7]. This so-called matrix effect was related to the speed of sample erosion by sputtering. The stationary *volume* concentration $[Cs]_0^\infty$ at depth $z = 0$ from the receding surface was assumed to scale with the sputtering yield Y as $[Cs]_0^\infty \propto 1/Y$ [7]. Such a relation had been predicted by a simple model of high-fluence retention [10], here referred to as the 'sputter approximation'. The approach involved several restricting assumptions. (i) After coming to rest, implanted atoms are immobile, (ii) the sample has an unlimited capacity to retain implanted atoms which (iii) do not cause a change in sample properties. One of the many problems associated with the $1/Y$ concept is the lack of a justification for the implicit idea that near-surface Cs atoms retained in the sample can generate the work function changes associated with the observed negative ion yield enhancement.

To overcome the problems, it has been suggested that "negative ion yield enhancement under alkali ion bombardment requires diffusion of implanted atoms to the surface where some pile-up has to take place to produce the desired lowering of the work function" [11]. Bulk diffusion of Cs was invoked in another retention study [12]. Recently published work, however, continued to

* Tel.: +49 89 3187 2439; fax: +49 89 3187 2949.
E-mail address: wittmaack@helmholtz-muenchen.de

1387-3806/$ – see front matter © 2011 Elsevier B.V. All rights reserved.
doi:10.1016/j.ijms.2011.12.004

interpret experimental data on the basis of the $1/Y$ approach [13,14] or a variant thereof, involving the idea that agreement with experimental data can be achieved assuming the release of surplus Cs by (thermal) desorption [15]. Other attempts to quantify $[Cs]_0^\infty$ involved the use of X-ray photoelectron spectroscopy [15,16] or Auger electron spectroscopy [17]. Such measurements are not specific to atoms residing *on the surface* because, at standard take-off angles, the detected electrons may originate from depths up to several nanometers.

In essence, the sputter approximation [10] fails to reproduce experimental findings in two ways, (i) samples are much more rapidly saturated with implanted atoms than predicted and (ii) the observed stationary concentrations are much lower than $1/Y$ (or lower than $1/(1+Y)$, if data are discussed in terms of atomic fractions). A recent study [18] has shown a very simple way out of this dilemma. The suggested 'rapid relocation model' of high-fluence retention is rather attractive in that it involves merely a simple reinterpretation of the parameter Y in the sputter approximation. The idea behind this approach is that in course of implantation and sputtering there is not only an apparent (passive) transport of implanted atoms to the instantaneous surface, the natural consequence of sample erosion by sputtering; there must also be processes in action that cause real transport of implanted atoms in the direction of the surface. The forces driving the transport are currently not known in any detail. One conceivable source of unidirectional motion could the pressure established by implanted insoluble atoms [19] or aggregates (clusters). Exciting aspects of the relocation model include (i) the finding that the active transport can be described by a single parameter, the relocation efficiency Ψ_{rel}, and (ii) the ability to combine passive and active transport in a single new parameter, the sum $Y_{eff} = Y + \Psi_{rel}$, which replaces Y in the sputter approximation.

The purpose of this study was twofold. The first aim was to provide evidence that implanted Cs atoms are in fact actively relocated towards the receding surface. The second, even more important aim was to show that, temporarily, they become adatoms, thus being able to act in terms of lowering the work function of the sample. However, one has to consider the fact that there is a competition between Cs transport to and removal from the surface. This implies the need to verify that the balance between implantation and removal of Cs atoms is in fact established under stationary bombardment conditions.

2. Experiment

A home-made quadrupole based ion microprobe [20] served for SIMS depth profiling. A ca. 1 cm × 1 cm piece of n-type Si(1 1 1) was cut from a polished wafer, cleaned with methanol and rinsed with high purity water; the native oxide was not removed. The sample was bombarded with raster scanned beams of 4 and 12 keV Cs^+ primary ions at 2° off normal. The yields of negative and positive secondary ions were measured in separate runs, the energy analyzer being set for transmission of ions around the peak of the energy distributions. The extraction field strength amounted to only a few V/cm. This has the advantage that Cs build-up should be distorted very little, if any, in both the positive and the negative SIMS mode (by contrast, in magnetic sector field instruments like the Cameca IMS nf series, a change in polarity at an electric field strength of 10 kV/cm must be expected to cause pronounced differences in Cs adatom growth). The erosion rate, assumed to remain constant during Cs implantation, was calculated from the beam current (1 nA), the bombarded area (270 μm × 270 μm), and the known sputtering yields (1.6 and 2.4, respectively [21]).

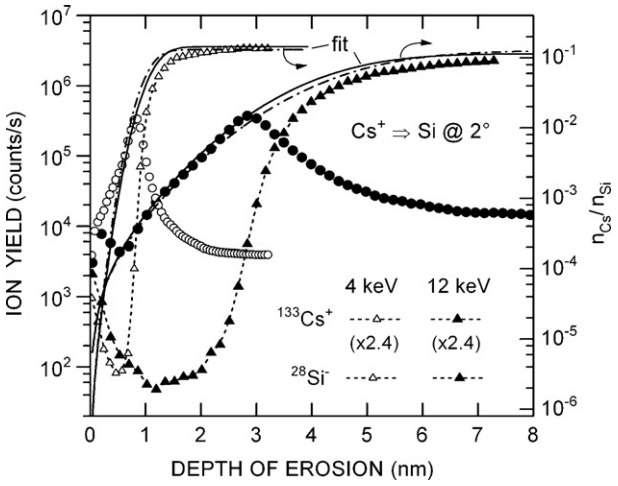

Fig. 1. Evolution of Si^- and Cs^+ secondary ion yields due to Cs implantation in Si at two different energies; left-hand scale. The dash-dotted and solid lines are fit functions for the pre-maximum Cs buildup, derived on the basis of the rapid relocation model; right-hand scale (see text). The calculated curves can serve to show that the fluence dependent build-up of the Cs^+ signals below the respective maxima is consistent with the final stages in the evolution of the Si^- signals.

3. Sputter yield calculations

Using the computer simulation program SRIM2006 (http://www.srim.org/) sputtering yields of Cs and Si, Y_{Cs} and Y_{Si}, respectively, were calculated for Cs impact on Si covered with Cs. The Cs coverage N_{Cs} was varied by selecting the corresponding mean thickness w_{Cs}. For the purpose in question here, sputter cross sections σ_{Cs} [22] were derived as $\sigma_{Cs} = Y_{Cs}/N_{Cs} = Y_{Cs}/w_{Cs}n_{Cs}$ (the number density of pure Cs, n_{Cs}, is 0.874×10^{22} cm^{-3}). The cross sections were found to be constant, i.e., independent of the Cs coverage, but only up to a thickness corresponding to about half a complete monolayer of Cs [23,24]. With a further increase in coverage, σ_{Cs} started to decrease, slightly first and then more rapidly. These changes are presumably a consequence of the large size of Cs atoms. The data discussed below fall into the region of constant (or almost constant) sputter cross section.

4. Results and discussion

Fig. 1 shows the build-up of Cs^+ and Si^- secondary ion yields. For ease of discussion the data are plotted as a function of the sputtered depth. The results reflect the well-known fact that the Si^- yield is strongly enhanced once the sample becomes sufficiently loaded with Cs. Concurrently, the Cs^+ yield first increases monotonically up to a maximum, then decreases significantly, to finally arrive at a stationary level. At the beginning of bombardment the Cs^+ profiles are distorted by some contamination which is attributed to cross contamination [25] generated during prior Cs bombardment of other areas on the analyzed sample. This contamination was removed after sputtering to a depth of 0.5 nm. The Si^- profiles are initially distorted by the presence of the native oxide. This aspect, however, is not relevant for the issue under study here.

According to low-fluence SIMS [3], the ionization probability of Cs^+ is constant at coverages below the yield maximum. As to dynamic SIMS, a very recent study [26] has shown that the constant (maximum) ionization probability in Cs^+ emission is observed only up to a Cs coverage of about 2×10^{13} cm^{-2}. In this region, the rapid relocation model was used to reproduce the observed build-up of the Cs^+ signals. In the Gaussian approximation [10], the fluence (φ) dependence of $[Cs]_0 \equiv n_{0,Cs}$, the predicted Cs number

density (concentration) at the receding surface ($z = 0$), relative to the Si concentration n_{Si}, reads

$$\frac{n_{0,Cs}(\varphi)}{n_{Si}} = \frac{1}{2Y_{eff}} \left\{ \mathrm{erf}\left(\frac{z_p}{\sqrt{2}\sigma}\right) + \mathrm{erf}\left(\frac{Y_{eff}\Omega_{Si}\varphi - z_p}{\sqrt{2}\sigma}\right) \right\} \quad (1)$$

$\Omega_{si} = {n_{si}}^{-1}$ denotes the atomic volume of Si atoms. The most probable ranges z_p, set equal to mean projected range $\langle z \rangle$, and the range straggling σ were calculated with SRIM (for 4 and 12 keV Cs: $\langle z \rangle = 8.3$ and 14.2 nm, $\sigma = 1.9$ and 3.7 nm, respectively).

For each of the two energies, two examples of calculated Cs build-up curves $n_{0,Cs}/n_{Si}$ are shown in Fig. 1, with Y_{eff} differing by 10% (4 keV: 11.5 and 12.6; 12 keV: 7.9 and 8.6, solid and dash-dotted lines, respectively). Finding the optimum (narrow) range of possible values for Y_{rel} was easy for the 12 keV data (optimum $\sigma = 4.3$ nm), but even for 4 keV the uncertainty does not exceed ± 15%. Note that $Y_{eff} \cong 12$ for 4 keV means that the implanted Cs atoms were a factor of $Y_{eff}/Y = 12/1.6 = 7.5$ more rapidly relocated to the receding surface than by pure sputter erosion. This result implies that a rather strong driving force existed that caused very efficient Cs transport.

The derived values of $n_{0,Cs}$ however, should be considered merely the *source* of active Cs atoms. In order to be effective for the purpose of interest, they must be converted to adatoms. The good fit of $n_{0,Cs}$ to the (pre-maximum) Cs^+ yields in Fig. 1 may be interpreted as saying that conversion of near-surface bulk Cs atoms to adatoms is fast, occurring 'immediately' on the time scale of the experiment, i.e., from one scan to the next. A simple estimate shows that the arrival rate of Cs atoms at the surface, represented by $n_{0,Cs}$, suffices to generate the Cs coverage required for strongly reducing the work function. Assume that the source of adatoms has a thickness corresponding to two layers of Si, equivalent to 2.7×10^{15} Si atoms/cm^2. With $n_{0,Cs}/n_{Si} = 0.1$, the source of Cs adatoms thus contains 2.7×10^{14} Cs atoms/cm^2, sufficient to change the work function by more than −3 eV (see below).

First evidence for the formation of Cs adatom layers was derived from a comparison of stationary implantation profiles of Xe and Cs, measured by Rutherford backscattering spectrometry, RBS [27]. However, the energy resolution was too poor to identify finer details of the Cs profile. Much improved depth resolution was achieved by medium energy ion scattering, MEIS [28,29], to the end that the measured spectra revealed a Cs adatom peak quite well separated from the distribution of Cs retained in the Si substrate. Of particular importance are the results reported for in situ MEIS analysis [28] of a sample saturated with Cs by bombardment with 5 keV Cs at 45°. The measured spectrum is reproduced schematically in Fig. 2(a), for clarity with more ideal separation than in the original experiment. The MEIS spectrum of a sample produced under very similar conditions (5.5 keV @ 42°), but analyzed only after intermediate sample storage in air [29], showed an adatom layer with an areal density higher by a factor 3.7 ± 0.5 than the sample analyzed in vacuum [28] (ca. 3.3 vs 0.9×10^{14} cm^{-2} by data reanalysis). This implies significant transport of Cs to the surface *after* completion of the implantation process, an aspect that deserves further studies.

A schematic drawing of the anticipated distribution of Cs atoms in Si is presented in Fig. 2(b), which is also meant to illustrate the very large difference in size between projectile and target atoms. The number of Cs atoms was chosen to comply with the profile of Fig. 2(a). Owing to the high Cs concentrations, here about 4 at% (i.e., much beyond the limit of solid solubility), it must be expected that the implanted atoms form aggregates or clusters, in analogy to bubbles produced by rare gas implantation [30]. Cluster integrity requires that (most of) the atoms in the Cs aggregates are neutral. The accumulation of the huge Cs atoms can be expected to exert tremendous stress that calls for relief. The most natural response of the target will be trying to get rid of the implanted atoms, as efficiently as possible. Vacancies generated by ion bombardment are likely to assist transport to the surface. Intuitively one would expect relief of stress to be easier the closer the implanted atoms have already come to the surface, in accordance with the results of Fig. 1.

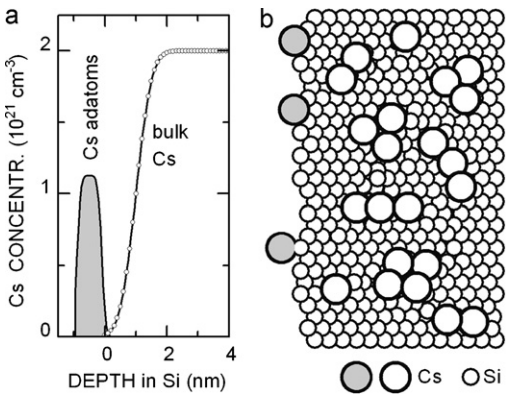

Fig. 2. (a) Stationary near-surface distribution of Cs in and on Si, generated by fully loading the sample with 5 keV Cs at 45°. Idealized profile based on data obtained by in situ MEIS analysis [28]. (b) Schematic illustration of the distribution of Cs atoms and clusters in Si (large open circles) and of Cs transferred to the surface (gray circles).

To proceed, we need reliable data for the stationary areal density of Cs adatoms. Using MEIS, this may be accomplished in dedicated future studies. At this point, the favored data must be derived along a more complex route. Following Yu [2,3], several groups have reported secondary ion yields as a function of the work function change $\Delta\Phi$ generated by sample loading with Cs. The vacuum level of the sample, measured with respect to the mass spectrometer, also changes by $\Delta\Phi$. This gives rise to a commensurate shift of the energy (spectra) of secondary ions which can be measured quite accurately in certain types of SIMS instruments [9,14].

Now the important but very reasonable idea is introduced that $\Delta\Phi$ should be independent of the method by which the Cs coverage is produced, whether by vapor deposition or by conversion of implanted atoms to the adatoms. Hence we can use available data for $\Delta\Phi(N_{Cs})$ to determine $N_{Cs}(\Delta\Phi)$. Five sets of Cs induced work function changes for Si(1 1 1) and Si(1 0 0) [31–33] are compiled in the main body of Fig. 3, deliberately presented in inverted form to generate the fit function $N_{Cs}(\Delta\Phi)$ used for the conversion of $\Delta\Phi$ to N_{Cs}, as described below. The data were obtained by Cs vapor deposition [32,33] or by exposure of the sample to a beam of Cs^+ ions of very low energy (<8 eV), producing no implantation [31]. The good agreement between the data from different sources is partly due to the fact that the Cs coverage quoted in the original publications was rescaled by constant factors to the end that the maximum achievable coverage agreed with the number determined quantitatively by RBS [23,24]. The solid lines in Fig. 3 represent third-order polynomial fit functions to the experimental data up to the observed maximum lowering of the work function.

According to results derived by thermal desorption spectrometry [32], the desorption energy E_d for Cs on Si depends strongly on coverage, see inset of Fig. 3. This behavior is due to the fact that the character of Cs–Si binding changes smoothly from purely ionic at the lowest coverage to Cs-like metallic near full monolayer coverage. In sputtering yield calculations the surface binding energy E_s is commonly set equal to the sublimation energy of the bulk material. Hence there is good reason to set $E_s = E_d$ for sputtering of adsorbed Cs.

Sputter cross sections were calculated with SRIM-2006, with $E_{s,Cs}$ as a variable. As an example, Fig. 4(a) depicts results for Si covered with 0.1 nm of Cs ($N_{Cs} = 0.87 \times 10^{14}$ cm^{-2}), bombarded

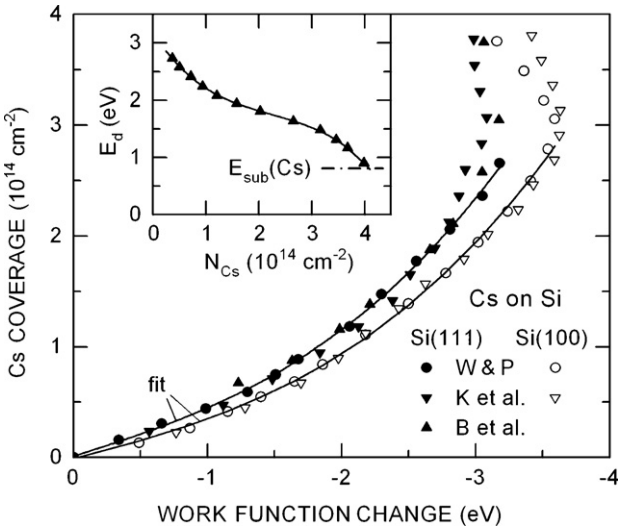

Fig. 3. Compilation of work function changes due to the deposition of Cs on Si(1 1 1) and Si(1 0 0) [31–33]. Compared to standard ways of data presentation, the *x*- and *y*-scales are exchanged, for reasons explained in the text. Inset: desorption energy vs Cs coverage [32].

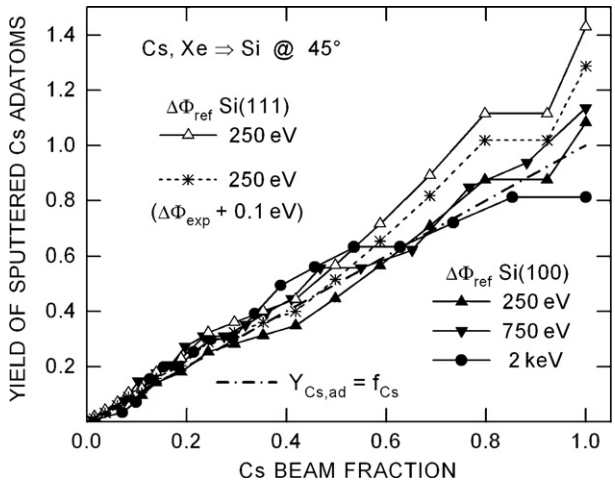

Fig. 5. Calculated sputtering yield of Cs adatoms reemitted from Si by mixed Cs/Xe bombardment at different energies vs the Cs fraction in the mixed beam. Full symbols: reference Si(1 0 0), open triangles: Si(1 1 1). The asterisks denote the sensitivity of the evaluation to a 0.1-eV difference in work function change compared to the data represented by open triangles. The 1:1 correspondence is represented by the dash-dotted line.

with 750 eV Cs at 45° (solid line: second-order polynomial fit). For $E_{s,Cs} > 1.5$ eV, σ_{Cs} varies as $1/E_{s,Cs}$. Additional simulations performed at impact energies between 0.25 and 12 keV and at impact angles of 0°, 42° and 45° revealed the systematic picture shown in Fig. 4(b). It turned out that the reduced sputter cross section, $\sigma_{Cs}E_{s,Cs}/Y_{Si}$, is largely independent of the bombardment parameters. The result is reasonable because the collision cascades initiated by ion impact serve to eject both the Si substrate atoms and the Cs adatoms. In quantitative terms, the simple picture needs to be refined whenever the energy distribution of sputtered atoms is increasingly truncated on its high-energy side. Ongoing studies (TRIM simulations; collaboration with A. Mutzke, to be published) have shown that this happens primarily for the following bombardment conditions: (i) large projectile-to-target mass ratio (as in the case of Cs on Si), (ii) low impact energy and (iii) more so the smaller the impact angle, i.e., the effect is most pronounced at normal incidence. Hence, the observation, in Fig. 4(b), that the scaled cross section for 750 eV

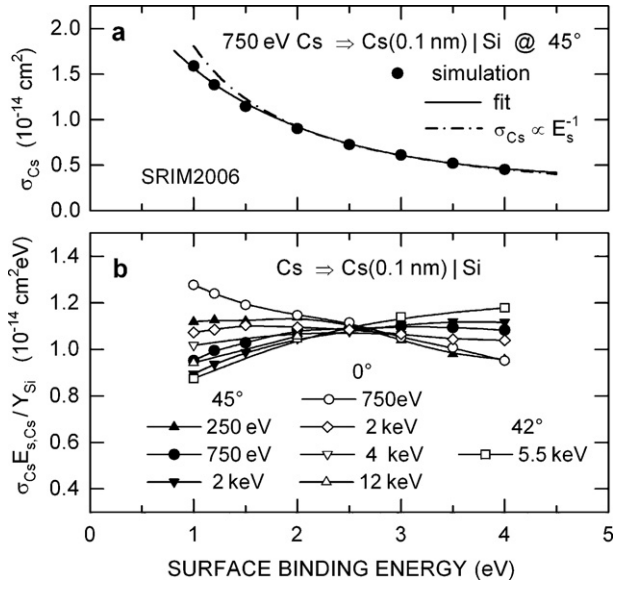

Fig. 4. (a) Sputter cross section and (b) reduced sputter cross section for removal of Cs adatoms from Si vs the Cs surface binding energy.

@ = 0° increases with decreasing surface binding energy, should be attributed to an unusually low sputtering yield Y_{Si}, the reason being that the collision cascades arriving at the surface contain an unusually small fraction of atoms that are capable to overcome the comparatively high binding energy of target atoms (4.7 eV). By contrast, the available energy suffices to eject Cs adatoms bound with energies <2 eV at fairly 'normal' rate. More details will be discussed elsewhere. Here it suffices to note that in cases where the absolute value of sputtering yields derived by SRIM may be considered debatable [34], the scaling behavior documented in Fig. 4(b) offers the possibility to replace calculated Y_{Si}-values by measured data.

With all required information at hand, we are now in the position to examine the balance between Cs adatom production and subsequent sputter removal. Use is made of $\Delta\Phi$-data reported by Brison et al. [14] for Si bombarded alternately with Cs^+ and Xe^+ ions, both incident at 45°. To vary the stationary sample loading with Cs, the ratio of the Cs^+ current to the sum of the two currents was varied between 0 and 1. This ratio defines the Cs fractions, f_{Cs}, in the mixed Cs/Xe beam. Note that Cs and Xe atoms have almost the same mass and, hence, produce essentially the same sputtering yield (of the same Cs loaded target). Depending on f_{Cs} and the beam energy, varied between 250 eV and 2 keV, the measured $\Delta\Phi$-values ranged between 0 and about −3.4 eV [14].

The $\Delta\Phi$-data of Ref. [14] were first converted to N_{Cs} using the fit functions according to Fig. 3. Knowing N_{Cs}, the surface binding energy $E_{s,Cs}$ could be determined from the data in the inset of Fig. 3. On this basis, σ_{Cs} was calculated. The sputtering yield of Cs adatoms was then determined as $N_{Cs}\sigma_{Cs}$. The results are compiled in Fig. 5 as a function of f_{Cs}. If Cs surface atoms were removed at the same rate as Cs ions were implanted, the data should fall on a straight line with unit slope. In fact, the solid symbols scatter around the dash-dotted line representing a 1:1 correspondence. It is important to note that the rapid decrease of E_d with increasing coverage (see inset of Fig. 3) provides a 'self-limitation' that prevents Cs overload: the higher the coverage, the larger the sputter cross section and the Cs removal rate.

There is some uncertainty as to the choice of the appropriate set of $\Delta\Phi$-data in Fig. 3, those for Si(1 1 1) or for Si(1 0 0). The latter case was given preference because the maximum $\Delta\Phi$-changes for Si(1 1 1) amount to only about −3.2 eV, less than the maximum of about −3.4 eV reported by Brison et al. [14]. However, for the sake of completeness, one example is included showing results on the basis

of $\Delta\Phi$ for Si(1 1 1), open triangles. The same data serve to illustrate the sensitivity of the evaluation to an absolute uncertainty of $\Delta\Phi$ by 0.1 eV.

The 1:1 correspondence documented in Fig. 5 has the important consequence that most, if not all implanted Cs ions are transiently converted to adatoms before they are finally removed by the action of the incident beam. Otherwise the calculated sputtering yield of Cs adatoms would be smaller than the Cs fraction in the mixed beam. Only when residing on the sample surface for a certain period of time, Cs atoms can produce a lowering of the work function. This constitutes a very efficient use of implanted Cs atoms for the desired purpose. Owing to the combination of two features, sputter ejection of Cs atoms buried in the sample contributes little to the balance between implantation and removal, (i) the mean depth-of-origin of sputtered atoms is only on the order of one or two monolayers of Si [35] and (ii) the Cs concentration in this near-surface region (inside the sample) is very low, as sketched in Fig. 2(a).

5. Conclusion

This study has shown that one can bridge the long lasting gap between secondary ion yield measurements at low fluence on samples with sub-monolayer quantities of deposited alkali atoms and dynamic (high fluence) studies involving sample bombardment with Cs primary ions. The resulting picture is simple and internally consistent: Cs induced secondary ion yield changes are generally produced by Cs atoms residing *on* the sample surface. In dynamic SIMS the residence time of adatoms may be short, depending on the bombardment parameters (primary ion energy, impact angle and mean current density). The finer details of Cs atom transport to the surface still need to be explored, including the time scale of the process.

Acknowledgements

I thank J. Brison and L. Houssiau for access to the raw data evaluated in Fig. 5.

References

[1] A. Kiejna, K.F. Wojciechowski, Prog. Surf. Sci. 11 (1981) 293.
[2] M.L. Yu, Phys. Rev. Lett. 47 (1981) 1325.
[3] M.L. Yu, Phys. Rev. B 29 (1984) 2311.
[4] T. Wirtz, B. Duez, H.-N. Migeon, H. Scherrer, Int. J. Mass Spectrom. 209 (2001) 57.
[5] P. Philipp, T. Wirtz, H.-N. Migeon, H. Scherrer, Int. J. Mass Spectrom. 264 (2007) 70.
[6] H.A. Storms, K.F. Brown, J.D. Stein, Anal. Chem. 49 (1977) 2023.
[7] V.R. Deline, W. Katz, C.A. Evans, P. Williams Jr., Appl. Phys. Lett. 33 (1978) 832.
[8] K. Wittmaack, Surf. Sci. 126 (1983) 573.
[9] H. Gnaser, Int. J. Mass Spectrom. Ion Processes 174 (1998) 119.
[10] F. Schulz, K. Wittmaack, Radiat. Eff. 29 (1976) 31.
[11] K. Wittmaack, Physica Scripta T 6 (1983) 71.
[12] W. Carr, M. Seidl, G.S. Tompa, A. Souzis, J. Vac. Sci. Technol. A 5 (1987) 1250.
[13] P.A.W. van der Heide, C. Lupu, A. Kutana, J.W. Rabalais, Appl. Surf. Sci. 231–232 (2004) 90.
[14] J. Brison, N. Mine, S. Poisseroux, B. Douhard, R.G. Vitchev, L. Houssiau, Surf. Sci. 601 (2007) 1467.
[15] B. Berghmans, B. Van Daele, L. Geenen, T. Conrad, A. Franquet, W. Vandervorst, Appl. Surf. Sci. 255 (2008) 1316.
[16] P.A.W. van der Heide, Surf. Sci. 447 (2000) 62.
[17] J. Brison, J. Guillot, B. Douhard, R.G. Vitchev, H.-N. Migeon, L. Houssiau, Nucl. Instrum. Methods Phys. Res. B 267 (2009) 519.
[18] K. Wittmaack, Nucl. Instrum. Methods Phys. Res. B 267 (2009) 2846.
[19] A. Mutzke, W. Eckstein, Nucl. Instrum. Methods Phys. Res. B 266 (2008) 872.
[20] K. Wittmaack, Surf. Sci. 345 (1996) 110.
[21] K. Wittmaack, J. Vac. Sci. Technol. A 3 (1985) 1350.
[22] K. Wittmaack, Surf. Sci. 89 (1979) 668.
[23] W.B. Sherman, R. Banerjee, N.J. DiNardo, W.R Graham, Phys. Rev. B 62 (2000) 4545.
[24] W.B. Sherman, R. Banerjee, N.J. DiNardo, W.R Graham, Surf. Sci. 479 (2001) 136.
[25] K. Wittmaack, Appl. Phys. A 38 (1985) 235.
[26] K. Wittmaack, Surf. Sci. 606 (2012), L18.
[27] N. Menzel, K. Wittmaack, Nucl. Instrum. Methods Phys. Res. 191 (1981) 235.
[28] R. Valizadeh, J.A. van den Berg, R. Badheka, A. Al Bayati, D.G. Armour, Nucl. Instrum. Methods Phys. Res. B 64 (1992) 609.
[29] A. Mikami, T. Okazawa, Y. Kido, Jpn. J. Appl. Phys. 47 (2008) 2234.
[30] K. Wittmaack, H. Oppolzer, Nucl. Instrum. Methods Phys. Res. B 269 (2011) 380.
[31] R.E. Weber, W.T. Peria, Surf. Sci. 14 (1969) 13.
[32] G. Boishin, M. Tikhov, M. Kiskinova, L. Surnev, Surf. Sci. 261 (1992) 224.
[33] T. Kan, K. Mitsukawa, T. Ueyama, M. Takada, T. Yasue, T. Koshikawa, Surf. Sci. 460 (2000) 214.
[34] K. Wittmaack, J. Appl. Phys. 96 (2004) 2632.
[35] K. Wittmaack, Phys. Rev. B 56 (1997) R5701.